UNIQUE ACHODRITE DHOFAR 778: A MANTLE-DERIVED FRAGMENT FROM A NEW DIFFERENTIATED BODY? R. L. Pang[1], W. Du[1,2], A. C. Zhang[2,3], J. Liu[2,4], and L. Qin[2,4]. [1]State Key Laboratory of Ore Deposit Geochemistry, Institute of Geochemistry, Chinese Academy of Sciences, Guiyang 550081, China (pangrunlian@mail.gyig.ac.cn). [2]CAS Center for Excellence in Comparative Planetology, Hefei, Anhui 230026, China. [3]State Key Laboratory for Mineral Deposits Research, School of Earth Sciences and Engineering, Nanjing University, Nanjing 210023, China. [4]CAS Key Laboratory of Crust-Mantle Materials and Environments, School of Earth and Space Sciences, University of Science and Technology of China, Hefei 230026, China.

Introduction: Dhofar 778 was an achondritic meteorite found in the desert of Oman in 2000. It was classified as a diogenite [1]. Oxygen isotopic study showed that Dhofar 778 has a $\Delta^{17}O$ value of −0.160±0.054‰ (2σ), which is different from that of Howardite-Eucrite-Diogenite meteorites (HED, −0.240±0.012‰, 2σ), suggesting that Dhofar 778 might be an anomalous diogenite [2]. Detailed studies of this anomalous achondrite are needed to explore its possible relationship with the other two anomalous eucrites with similar oxygen isotopic compositions, Dhofar 007 (−0.173±0.01‰, 2σ) and NWA 12338 (−0.18 ±0.01‰, 2σ) [2–4]. In this study, we report the petrographic, mineralogical, and geochemical results of Dhofar 778, which would be helpful in constraining its petrogenesis and understanding the melting and differentiation of the planetesimal sampled by Dhofar 778.

Analytical methods: Petrographic investigations were performed by using FE-SEM (FEI FIB-SEM at the Institute of Geochemistry; Zeiss Supra 55 at Nanjing University). TEM investigations were carryout out at FEI Tecnai F20 at Nanjing University. Mineral compositions were analyzed with EPMA (JXA 8230 at the Institute of Geochemistry and JEOL 8100 at Nanjing University). Laser Raman spectra and trace element compositions were obtained at the Institute of Geochemistry with Renishaw in Via, and Plasma Quant MS Elite ICP-MS, respectively. Chromium isotopic analyses were carried out by Thermo Scientific TRITON Plus TIMS at University of Science and Technology of China (methods in [5])

Results & Discussion: Dhofar 778 is fragmental with intriguing shock veins. The brown coloration of Dhofar 778 is due to the rusting of FeNi metal and shock-darkening of olivine, which is similar to those in shocked martian meteorites [6].

Petrography and mineralogy. Dhofar 778 consists mainly of orthopyroxene (~54 vol%) and olivine (~44 vol%), justifying it as a harzburgitic achondrite (Fig. 1a). It can be divided into poikilitic and non-poikilitic regions and orthopyroxene is dominant in the former. Olivine ($Fo_{71–74}$, Fe/Mn=46 ± 3) is homogeneous, whereas orthopyroxene shows profound Fe-Mg zoning ($En_{71–87}Fs_{13–24}Wo_{0.4–4.5}$, Fe/Mn =29±4) (Fig. 1a). Other phases (~2 vol%) include plagioclase ($An_{72–93}$), pigeonite ($En_{74–76}Fs_{23–24}Wo_{6-8}$), augite ($En_{47–51}Fs_{11–14}Wo_{36–41}$), chromite ($Chr_{63–82}Spl_{16–35}Usp_{1–4}$), troilite, FeNi metal (7–18 wt%Ni), and silicic glass (87–93 wt%SiO_2).

Coarse olivine grains up to 5 mm in size are observed. They usually contain orthopyroxene-spinel intergrowths (Fig. 1b). Similar symplectic intergrowths have been observed in terrestrial, martian, lunar and asteroidal olivine [7]. Various models have been proposed to interpret their formation, including reaction of olivine with melt, crystallization of trapped interstitial melt, metasomatism by the chromite-saturated melt, and dehydration of OH-bearing local domains in olivine [7]. The highly silicic glass occurs exclusively as inclusions in olivine. Silicic inclusions have been reported in some achondritic meteorites (e.g., Chassigny and Luna-24 samples), and mechanisms such as partial melting, fluid precipitation, liquid immiscibility, and residual origin have been proposed for their formation [8]. However, our current data do not suffice to determine the formation mechanisms of the orthopyroxene-spinel intergrowths and silicic glass in Dhofar 778.

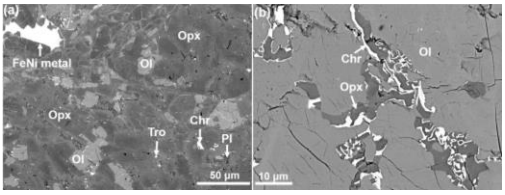

Fig. 1. Representative BSE images of Dhofar 778 (a) and the intergrowths of orthopyroxene-chromite in olivine (b). Ol = olivine; Opx = orthopyroxene; Chr = chromite; Tro = troilite; Pl = plagioclase.

Shock metamorphism. The olivine grains that are trapped or in the vicinity of shock veins have been transformed into ringwoodite and wadsleyite (Fig. 2a). Phase diagram of Mg_2SiO_4-Fe_2SiO_4 system suggests a shock pressure of ~13−17 GPa (1200−1600 ℃) [9].

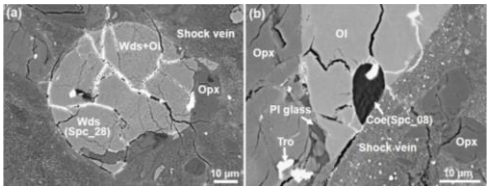

Fig. 2. BSE images of wadsleyite (a) andcoesite (b). Wds = wadsleyite; Coe = coesite; Chr = chromite; Tro=troilite; Pl glass = plagioclase glass.

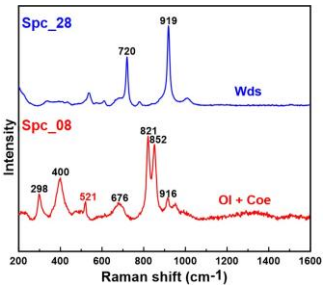

Fig. 3. Raman spectra of wadsleyite and the likely coesite.

Trace element compositions: Trace element abundances of Dhofar 778 and Dhofar 007 are illustrated in Fig. 4. The Ni contents in Dhofar 778 (868 µg/g) and Dhofar 007 (877 µg/g) are significantly high, which are consistent with the previous study (929±32 µg/g, [3]) and our observations (Fig. 1a). The REE abundances of Dhofar 007 in this study are higher than that in [3], indicating the heterogeneity of lithology in Dhofar 007. Dhofar 778 has a "U-shaped" profile (Fig. 5), which resembles that of the terrestrial harzburgites with high modal of orthopyroxene [10]. However, the enrichment of all REE (1.04–1.78 × chondrite) in Dhofar 778 is significantly different from [10]. The LREE enrichment in [10] is caused by fluid-assisted melt-rock interaction, whereas the LREE enrichment in Dhofar 778 might be affected by terrestrial weathering.

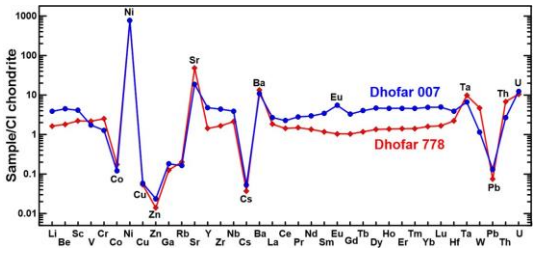

Fig. 4. Chondrite-normalized multi-elements of Dhofar 778 and Dhofar 007. The CI chondrite data are from [11].

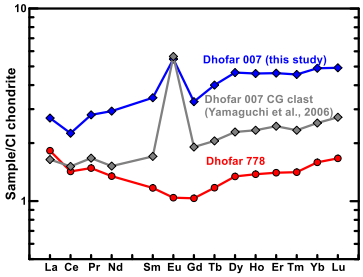

Fig. 5. Chondrite-normalized bulk REE abundances of Dhofar 778 and Dhofar 007 in this study. The REEs of Dhofar 007 coarse-grained granular (CG) clast are from [3].

Cr isotopic composition: The ε^{54}Cr values of Dhofar 778 and Dhofar 007 are -0.51 ± 0.07 (2σ), -0.46 ± 0.09 (2σ), respectively, which are slightly higher than that of typical HED meteorites and slightly lower than that for the anomalous eucrites (except NWA 1240, Fig. 6). Considering the much lower Cr content of the upper continental crust (averaging 92 ppm, [12]) than our samples (6568 ppm Cr in Dhofar 778; 3364 ppm in Dhofar 007), the effect of terrestrial contamination on ε^{54}Cr is minimal. The overlapping ε^{54}Cr between Dhofar 778 and Dhofar 007 suggests a possible genetic link between them. However, more high-precision oxygen isotopic analyses await to proceed due to the large uncertainties in current oxygen isotope composition of Dhofar 778 and the unsolved questions about distinct oxygen compositions in Dhofar 007 [2]. It is not clear whether the isotopic heterogeneity is correlated to the distinct lithology.

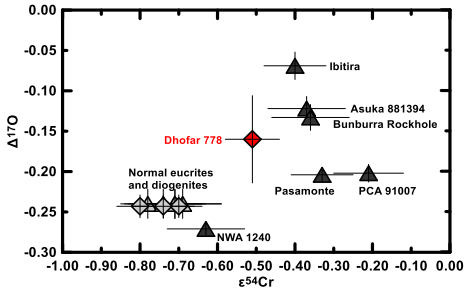

Fig. 6. Δ^{17}O-ε^{54}Cr plot. Oxygen isotope data of Dhofar 778 (red), and normal HED meteorites (light gray) are from [2]. ε^{54}Cr data of the normal meteorites are from [13] and that of anomalous eucrites (dark gray) are from [14] and [15].

Conclusions: Dhofar 778 is a harzburgitic achondrite that is isotopically distinct from typical HED meteorites. It might be a fragment from the mantle of a newly found differentiated body. The link between Dhofar 778 and anomalous Dhofar 007 is likely and warrants further investigation.

Acknowledgments: We thank Thomas Vettori for providing the Dhofar 778 meteorite and Mike Lippold for preparing the thin section.

References: [1] Russell S. S. et al. (2003) *Meteoritics & Planet. Sci., 38*, A189–248. [2] Greenwood R. C. et al. (2017) *Geochem., 77*, 1–43. [3] Yamaguchi A. et al. (2006) *Meteoritics & Planet. Sci., 41*, 863–874. [4] Guo Z. et al. (2019) *50th LPSC*, Abstract #1583. [5] Qin L. P. et al. (2010) *Geochim. Cosmochim. Acta*, *74*, 1122–1145. [6] Takenouchi A. et al. (2018) *Meteoritics & Planet. Sci., 53*, 2259–2284. [7] Khisina N. R. and Lorenz C. A. (2015) *Petrology, 23*, 176–188. [8] Varela M. E. *Meteoritics & Planet. Sci., 33*, 1041–1051. [9] Tomioka N. and Miyahara M. (2017) *Meteoritics & Planet. Sci., 52*, 2017–2039. [10] Secchiari A. et al. (2020) *Geosci. Front., 11*, 37–55. [11] Barrat J. A. et al. (2003) *Geochim. Cosmochim. Acta*, *73*, 3959–3970. [12] Rudinick R. L. and Gao S. (2003) *Treatise Ceochem., 3*, 1–62. [13] Trinquier A. et al. (2007) *Astrophys. J., 655*, 1179. [14] Benedix G. K. et al. (2017) *Geochim. Cosmochim. Acta, 208*, 145–159. [15] Sanborn M. E. and Yin Q. Z. (2014) *45th LPSC*, Abstract #2018.